A Hyperspectral Imaging Spectral Unmixing and Classification Approach to Pigment Mapping in the Gough & Selden Maps

Di Bai[a]* and David W. Messinger[a] and David Howell[b]

[a]*Chester F. Carlson Center for Imaging Science, Rochester Institute of Technology, Rochester, New York, USA;* [b]*Bodleian Library, University of Oxford, Oxford, UK*

Contact Di Bai. Email: db3641@rit.edu

In this research, a spectral unmixing and classification approach for hyperspectral imagery (HSI) of historical artifacts is introduced. The Gram Matrix and MaxD techniques have been used to estimate the within material diversity in a HSI and extract the spectra of the class exemplars, called endmembers. Due to the absence of ground truth, the exemplar spectra are assumed to represent pure materials in the scene or unique pigment mixtures. After extracting endmembers, the Nonnegative Linear Least Squares algorithm and the K-means algorithm are then used to classify the HSI based on the endmembers. We also proposed a "spectral angle spatial patterns" method to map the class membership and goodness across the map to identify per-class spatial patterns. This approach has been successfully utilized in two historical artifacts, the Gough Map of Britain (c.1400) and the Selden Map of China (c.1619). Both maps were imaged using a hyperspectral imaging system while in the collection at the Bodleian Library, Oxford University. It reveals at least six kinds of dominant water pigments used in each map along with their spatial distribution. This approach can be generalized to a novel pigment mapping tool for historical geographers to analyze the material diversity of historical artifacts.

Keywords: hyperspectral imagery; spectral unmixing; pigment mapping; dimensionality estimation; endmember analysis; historical artifacts; nonnegative linear least squares; material diversity.

1. Introduction

The Gough Map, dating from the 15th century (Solopova 2012; Lilley, Lloyd, and Campbell 2009; Delano-Smith et al. 2016; MILLEA 2007), is one of the earliest surviving maps of Britain. The substrate of the map is a combination of approximately 1/4 lamb skin in the north and 3/4 sheepskin in the south. Over half of the map is drawn in green indicating the ocean, coastal areas and rivers. There are more than 600 towns in red and many thin red lines indicating the distances between the towns (Solopova 2012; Lilley, Lloyd, and Campbell 2009; Delano-Smith et al. 2016). Previous research revealed that the Gough Map was extensively revised after its creation (Solopova 2012; Delano-Smith et al. 2016). Specifically, south of Hadrian's Wall, most of the rivers and the coastline were overdrawn with a thicker nib and darker green ink (Solopova 2012). In 2015, the map was imaged using a hyperspectral system at the Bodleian Library, Oxford University. The goal of the collection includes faded text enhancement for reading and pigment analysis for estimation of material diversity in the Gough Map for codicological studies. To ensure full coverage with sufficient spatial resolution, the collection was done in six overlapping HSI “chips”. The size of each chip is 1600 (pixels) x 5512 (pixels) x 334 (bands). Its spectral range is from 400nm to 1000nm over the visible and near infrared (Vis-NIR). Section 3 introduces more collection details.

The Selden Map of China, dating from c.1619, was rediscovered at the Bodleian Library by Robert Batchelor in 2008 (Batchelor 2013, 2014; Nie 2014). This is not only a map of China (Ming Empire), but of the whole of East and Southeast Asia (Nie 2014), including China, Japan, Korea, Vietnam, the Indian Sea, Timor and the shipping routes from Indonesia to the western coast of India (Batchelor 2014; Nie 2014). It provides significant information to examine the history of Chinese cartography and analyze the maritime dimensions of Asia (Batchelor 2013). The map was drawn with carbon ink

and watercolours on a Chinese paper, including mountains, rivers, ocean waves, forests, plants and flowers. About six different colors were used: red, green, blue, yellow, white and black (Nie 2014). Specifically, the color green dominates this map due to the large areas of the sea in the map (Kogou et al. 2016). To analyze the pigment diversity of the Selden Map, researchers collected 12 HSIs of the Selden Map (full coverage of the entire map) at the Bodleian Library in 2015. The size of each chip varies from 1600 (pixels) x 2300 (pixels) x 334 (bands) to 1600 (pixels) x 3250 (pixels) x 334 (bands), with a spectral range from 400nm to 1000nm. Section 4 states more collection details.

Pigment analysis of the Gough Map and the Selden Map will contribute to the codicological studies of the maps (i.e., understanding the tools, techniques, and timeline of its creation and revision). Previous work on historical artifacts codicological studies mainly included faded text enhancement and pigment analysis. To enhance faded text, people used techniques such as multispectral reflectance imaging, fluorescence capturing, and transmission imaging (Easton, Barry, and Knox 2011; Easton and Noel 2010; Barry, Boydston, and Easton 2011, 2010; Easton, Knox, and Barry 2011; Knox et al. 2011; Easton and Kelbe 2014; Easton and Noel 2004; Easton et al. 2015). For example, Easton and his colleagues used a multispectral imaging system, called the Megavision Imaging System, to collect images of historical manuscripts such as the Herculaneum Papyri and Archimedes Palimpsest. Then they applied image segmentation, independent component analysis (ICA), principal component analysis (PCA), renderings in pseudo-color and spectral pseudoinverse calculation to enhance multi-spectral images of historical documents (Easton, Barry, and Knox 2011; Easton and Noel 2010; Barry, Boydston, and Easton 2011, 2010; Easton, Knox, and Barry 2011; Knox et al. 2011; Easton and Kelbe 2014; Easton and Noel 2004; Easton et al. 2015). For HSI analysis, Goltz (Goltz et al. 2010) used hyperspectral imaging to assess

stains on historical manuscripts. He calculated the minus log function of the image pixel value over the white reference to generate optical density slices of certain ranges of spectra and created false color images to enhance faded text.

For pigment analysis of historical artifacts, hyperspectral imaging had been used in material identification and mapping of works of art (Legrand et al. 2014; Fischer and Kakoulli 2006; Rosi et al. 2013; Dooley et al. 2013; Delaney et al. 2010, 2016; Bai, Messinger, and Howell 2017b,a), such as (a) estimating the timeline of a manuscript's creation and revision (Melessanaki et al. 2001), (b) differentiating pigments of historical paintings (Delaney et al. 2016; Liang 2012; Daniel et al. 2016; Baronti et al. 1998), (c) analyzing historic value of artworks (Melessanaki et al. 2001; Balas et al. 2003; Klein et al. 2008) and (d) studying of the methods used in the artifact creation (Attas et al. 2003). Researchers used different imaging system, such as laser induced breakdown spectroscopy (Melessanaki et al. 2001), infrared imaging (Casini et al. 1999; Cucci, Delaney, and Picollo 2016) and X-ray fluorescence imaging (Legrand et al. 2014; Delaney et al. 2016) to obtain imagery. Image processing techniques included dimensionality reduction, such as PCA (Dooley et al. 2013; Baronti et al. 1998; Attas et al. 2003) and image segmentation, such as spectral angle mapper (SAM) (Daniel et al. 2016), support vector machine (SVM) (Polak et al. 2017) and spectral unmixing (Liang 2012). Dooley et al (Dooley et al. 2013) and Delaney et al (Delaney et al. 2010) also used N-d visualizer in ENVI software to find endmember spectra and used SAM to classify pigments of HSI. In 2017, Bai et al (Bai, Messinger, and Howell 2017b, a) presented an approach by using the Gram Matrix and endmember analysis to estimate the red and green pigment diversity over the Gough Map. Then they used SAM to segment the HSI of the Gough Map into six different classes. That was the first attempt to estimate within material diversity in historical artifacts. Different from previous work

on segmentation of the HSI, within material diversity estimation focuses on specific regions (with common visual color) in a hyperspectral image. For example, the Gough Map is drawn with green and red pigments on a sheep/lamp skin. The goal of within material diversity estimation is to calculate how many distinct green (or red) pigments were used during its creation and revision, which is essential to the codicological studies of the maps (i.e., understanding the tools, techniques, and time-line of its creation and revision). It requires extraction of the green (or red) pigments/pixels from the HSI first (without affecting other pigments) and then process the data of only the green (or red) pigments.

The objective of this research is to extend Bai's research by using a spectral unmixing technique (NNLS) to estimate the diversity of the pigments used to denote water in the two maps, which are predominantly visually "green" in color. The contribution includes: (1) within material diversity (water pigments) estimation of two medieval maps, (2) testing a new method for this application, and (3) proposing a spectral angle spatial pattern analysis method to validate the classification results. Here, without ground truth we assume that the endmembers represent either a pure pigment or a mixture of pigments. We provide a mathematical way to extract exemplar spectra (endmembers) that can be used to model the remaining pixels in the image. Eventually, we find that there are at least six different kinds of pigments used to show water that are generally visually "green" in the Gough Map and six different "green" pigments in the Selden Map. The spatial patterns of different pigments indicate the construction and correction of this map. The source of those different pigments needs further chemical research in the future.

This paper is organized as follows. Section 2 describes the methodology including: 1) the material diversity estimation techniques, the MaxD & Gram Matrix, 2)

the NNLS spectral unmixing method and 3) spectral angle spatial patterns method. Section 3 introduces the application of estimating the material diversity of the water pigments in the Gough Map and presents the results. Section 4 describes the application of the Selden Map. Section 5 summarizes the results and findings.

2. Methodology

Pigment diversity estimation provides the endmembers of different materials within a HSI (i.e., their exemplar spectra). Then, a spectral unmixing technique, NNLS, is used to calculate the abundances of those endmembers in each pixel. After obtaining the abundance matrix for all pixels, the K-means method is used to classify this abundance matrix into different classes, which is then used as the label for each water pixel in the map. The methodology is outlined here:

(1) To reduce computation time, we cut each HSI chip of the Gough Map into top and bottom sub-chips, such as 1L(top). For the Selden Map, since there are fewer water pigments in each chip, we do not need to cut the HSIs.

(2) Extract water pixels from each HSI chip of the map.

   a. For the Gough Map, we use Mahalanobis distance classifier in ENVI software to classify each HSI chip into three classes, including red pixels (text & town signs), green pixels (the water) and background. We then create a binary mask of all the water pixels in each chip.

   b. For the Selden Map, due to the complexity of the pigments in the Selden Map, we need to use Photoshop (instead of using the Mahalanobis classification tool) to create a water pixels' mask of the Selden Map.

   c. Extract spectral information of all the water pixels from the water pixel mask and record the coordinates of each pixel accordingly.

(3) Hyperspectral data pre-processing:

   a. Sphere the data: normalize each pixel to a unit magnitude to eliminate brightness differences between the HSI chips.

   b. Bin the data: spectrally bin the data from 334 bands to 111 bands, so as to increase the signal to noise ratio (SNR).

(4) Estimate the dimensionality and compute endmembers for each chip using the Gram Matrix and MaxD techniques.

(5) Compute global endmembers of the water pigments across the entire map.

(6) Classify water (green) pixels per HSI chip.

   a. For each chip, use NNLS to compute the abundance matrix of the data.

   b. Use K-means to classify the abundance matrix (or the abundances + differences matrix) into certain classes and label each pixel accordingly.

   c. Map the results back to the image for visual interpretation.

(7) Compute average spectrum within each class and generate spectral angle spatial patterns of each class to validate the classification accuracy.

This section provides the detailed description of material diversity estimation techniques, the MaxD & Gram Matrix approaches, the spectral unmixing technique, nonnegative linear least squares (NNLS) (Lawson and Hanson 1995) and the method for assessing the quality of the resulting class map in the absence of ground truth. Details of other steps will be introduced in the results section.

2.1 Material Diversity Estimation

Material diversity estimation of a HSI can be related to the dimensionality estimation of the HSI in the spectral domain. The dimensionality estimation calculates the least number of free variables required to represent the data without losing information

(Camastra 2003). There have been many techniques used in dimensionality estimation of HSI datasets (Camastra 2003; Messinger et al. 2012; Canham et al. 2011; Kirby 2000; Jolli e 2002; Ziemann, Messinger, and Basener 2010; Yao and Qian 2009; Pettis et al. 1979). In this research, we use an approach developed by Messinger (Messinger et al. 2010) and applied by Canham (Canham et al. 2011) to estimate the water pigment diversity in the HSI of the Selden Map and the Gough Map. We use the MaxD technique to obtain endmembers and then use the Gram Matrix to estimate the dimensionality of data and determine how many endmembers to keep. MaxD algorithm defines a set of basis vectors that span the image space. By generating a subspace that large enough to contain the data but meanwhile small enough to reduce the dimensionality of its space, it seeks a simplex that encloses these spectral vectors and suppose that this simplex can be constructed from the extrema of the available HSI data. The Gram Matrix is a $k * k$ matrix, where k is the number of vectors in the data set. The (m, n) th element of the Gram matrix is the inner product of the m and n vectors in the data set, such that

$$G_{m,n} = \langle \overrightarrow{x_m}, \overrightarrow{x_n} \rangle \quad (1)$$

Note that the determinant of G is the square of the volume of the parallelepiped that encloses the vector set. A significant property of the Gram matrix is that if the Gram Matrix is composed of endmembers extracted from the data (as we do here), when the determinant of G approaches zero, the vectors in the data set are no longer linearly independent, which indicates the number of distinct materials in the data set. A simplified example of the volume estimation is illustrated in Fig. 1 using the volume of a cuboid. When the volume of a two-dimensional data set is calculated in three-dimensions, the volume is zero as the third dimension has zero "length". The same

approach applies to the endmember vectors as extracted from the high dimensional hyperspectral image. Fig. 2 depicts the estimated convex hull volume vs the number of endmembers of an example HSI chip of the Gough Map. Note that when the volume function approaches zero, the number of endmembers indicates the number of distinct materials in the HSI, here 6.

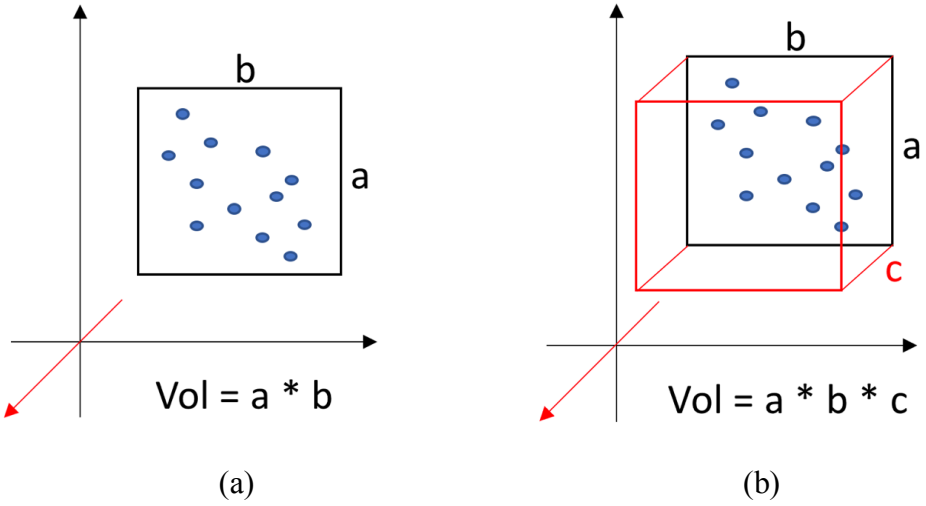

(a) (b)

Figure 1. Example of volume estimation in multiple dimensions. (a) Two-dimensional (2D) data with volume calculated in 2D. (b) 2D data with volume calculated in 3D.

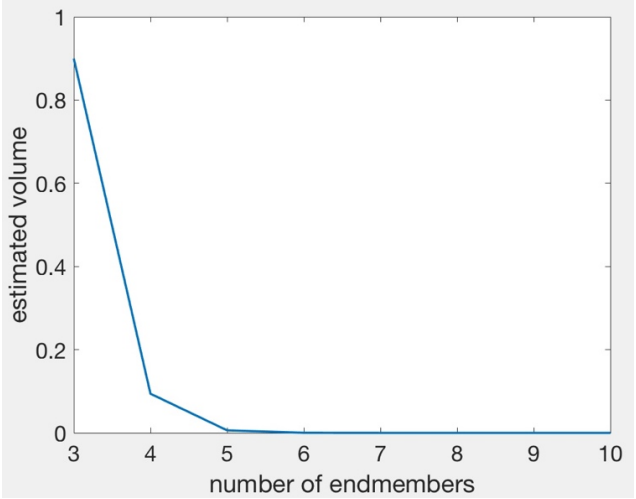

Figure 2. Material diversity plot for one HSI chip of the Gough Map with x axis: number of endmembers and y axis: estimated convex hull volume.

More details of this technique are in the literature (Messinger et al. 2010; Ziemann, Messinger, and Basener 2010; Messinger et al. 2012; Canham et al. 2011).

In this research, to reduce the computation time of the Gram Matrix, we divide each HSI of the Gough Map into top and bottom sub-chips. Since we are only working on water pigments, after extracting only the water pixels from each sub-chip, the size of each data matrix is less than 4 GB, which needs less than 5 minutes to compute the Gram Matrix. For the Selden Map, we don't need to divide each chip into sub-chips. Similarly, the size of each data matrix for the water pixels is also less than 4 GB.

The algorithm of Gram Matrix and MaxD are shown below.

(1) For each data matrix, we extract a (relatively) large number of endmembers, here $W \approx 15$, using the MaxD algorithm.
(2) MaxD orders the endmembers by overall magnitude, and we iterate k from 3 to W endmembers (at least three dimensions) using the MaxD:
    i. represent the k endmembers in the Gram matrix.
    ii. compute the convex hull volume for k endmembers from the determinant of G.
    iii. save the volume function of k.
(3) The dimensionality of the data is estimated by the number of endmembers where the volume function approaches zero.

2.2. Spectral Unmixing

Since we don't have the ground truth, or a reliable library of pigment spectra used in the map, the endmembers are assumed to represent pure materials in the scene. And endmembers can certainly represent a mixture of pigments. Here we provide a mathematical way to extract exemplar spectra that can be used to model the remaining

pixels in the image. We use nonnegative linear least squares (NNLS) (Lawson and Hanson 1995) to identify the abundances of those endmembers in each pixel (Heylen, Parente, and Gader 2014). Lawson and Hanson gave the standard algorithm for NNLS (Lawson and Hanson 1995). This algorithm solves a nonnegative least squares curve fitting problem by minimizing the objective function: $\min_x \left\| C * \vec{x} - \vec{d} \right\|_2^2$, where $\vec{x} \geq 0$. In this function, $\vec{d}$ is the reflectance vector of each pixel, C represents the endmember matrix and $\vec{x}$ is the abundances of those endmembers. Each column of the abundance matrix represents the abundances of six endmembers in one single pixel $\vec{x}$, such that the pixel $\vec{x}$ is written as:

$$\vec{x} = 0.605\vec{E_1} + 0.000\vec{E_2} + 0.201\vec{E_3} + 0.079\vec{E_4} + 0.048\vec{E_5} + 0.067\vec{E_6} \quad (2)$$

Here, $\vec{x}$ is a single pixel vector, whose abundance vector is shown in the first column. The number of columns represents the number of pixels. More details of this approach can be found in the literature (Chen and Plemmons 2010).

After obtaining the abundance matrix, generally, class labels are based on the endmembers with the highest abundance. For example, if we have two following pigments with the combination of three endmembers (materials):

Pigment 1: $\vec{x}_1 = 0.98\vec{E_1} + 0.01\vec{E_2} + 0.01\vec{E_3}$

Pigment 2: $\vec{x}_2 = 0.96\vec{E_1} + 0.02\vec{E_2} + 0.02\vec{E_3}$

Pigment 1 and Pigment 2 both consist of over 95% of the first endmember (material), so that apparently, we can classify these two pigments into the same class. But in this research, we are trying to estimate within material differences and the subtle differences between pixels are potentially a mixture of different endmembers. For example, we generally have pigments such as:

Pigment 3: $\vec{x}_1 = 0.44\vec{E_1} + 0.46\vec{E_2} + 0.10\vec{E_3}$

Pigment 4: $\vec{x}_2 = 0.14\overrightarrow{E_1} + 0.60\overrightarrow{E_2} + 0.26\overrightarrow{E_3}$

The largest abundance in Pigment 3 and 4 are both class 2 (since 0.46 > 0.44 > 0.10 and 0.60 > 0.26 > 0.14). However, those two cases have different combinations of the endmembers (materials) and should likely be placed into different classes. That's why we propose to compute the K-means classification to this abundance matrix and label each pixel based on the classification results. To differentiate those two cases, we first use K-means to classify the original abundance matrix and also add more descriptors, which are the differences between the abundances. Without knowledge of the truth, we simply create the best model of each pixel possible. To continue the example above, in Pigment 3, we will have (0.4 - 0.5), (0.4 - 0.1) and (0.5 - 0.1) as new features in the pixel descriptor. The abundance vector will be extended from [0.4, 0.5, 0.1] to [0.4, 0.5, 0.1, -0.1, 0.3, 0.4]. We call this new abundance matrix the "abundances + differences" matrix. Then we apply K-means classification to this new matrix and label each pixel accordingly. The "abundances+differences" approach aids in separating subtle differences between the pigment classes.

To estimate the global number of water pigments, for example, we compute Gram Matrix to the 72 primary endmembers from 12 sub-chips of the Gough Map (6 endmembers each). The result shows that there are 6 global endmembers. Then we use K-means to classify the 72 endmembers into 6 classes and compute average spectra within each class. After that, we perform spectral unmixing to get the abundance descriptors for each pixel.

2.3. Class Map Validation

Due to the absence of ground truth data, we generate spatial patterns of the spectral angle between each pixel and its class mean within each class to validate the

classification results. This provide a quantitative measure of how good the class labels are, relative to the mean class spectra, in the absence of ground truth. Consequently, if it was a poor classification, or a poor endmember extraction, these values would be high. This is simply proposed as a method of assessing confidence in the result when no per-pixel ground truth is available. The method is outlined below.

(1) Compute the average spectrum within each class and take that spectrum as the representative of this class.
(2) Compute spectral angle between each pixel and the representative of its assigned class.
(3) Replace each pixel's value by this spectral angle.
(4) Map the results back to the image for visual interpretation.

Spectral angle (Kruse et al. 1993) is defined as:

$$\theta(x, y) = \cos^{-1}\left(\frac{\sum_{i=1}^{n} \overrightarrow{x_i} * \overrightarrow{y_i}}{\left(\sum_{i=1}^{n} x_i^2\right)^{\frac{1}{2}} * \sum_{i=1}^{n} y_i^{2\frac{1}{2}}}\right) \quad (3)$$

where, in this case, $\vec{x}$ is the spectral vector of a water pixel, $\vec{y}$ is the spectral vector of an endmember, and n is the number of spectral bands (here n = 111).

The goal of this research is to estimate the number of distinct water pigments in the Gough Map and the Selden Map and provide a global distribution pattern of different water pigments, despite their common visually “green” appearance. This will hopefully aid in our understanding of how the artifacts were created and/or revised.

3. Results for the Gough Map

In this section, we will estimate the within material diversity of the water pigments in the Gough Map using the above techniques. The collection parameters of the HSI and the results will be introduced as follows.

3.1. Collection Parameters

The Gough Map, shown in Figs. 3(a) & 3(b), is drawn on a combination of one piece of sheepskin and one lambskin, but the sewing is hardly seen (MILLEA 2007). The size of the Gough Map is 55.3 x 116.4cm with a scale at about 1: 1,000,000. To ensure full coverage of the map with sufficient spatial resolution, the Gough Map was imaged in six spatially overlapping chips and labelled as 1L(left), 1R(right), 2L, 2R, 3L and 3R from bottom to top, as shown in Fig. 3(c), Each HSI chip has 334 bands with a spatial size of 1600 x 5512 (pixels). The entire map is about 3743 x 8987 (pixels). Given the actual size of the Gough Map is 55.3 x 116.4 cm, the spatial resolution is $\Delta y \approx 68$ pixels/cm (0.015 cm/pixel) vertically and $\Delta x \approx 77$ pixels/cm (0.013 cm/pixel) horizontally. In addition, each chip has 334 bands over the visible and near infrared (Vis-NIR) range from 398.7 nm to 1000.3 nm, so that $\Delta\lambda = 1.8$ nm.

(a)

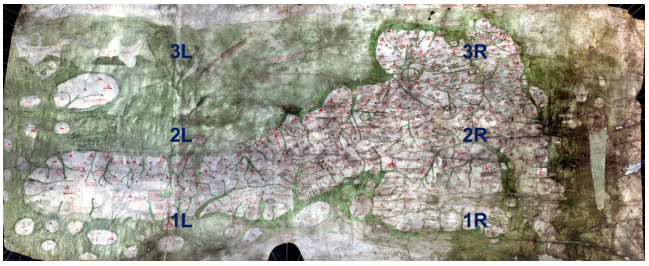

(b) (c)

Figure 3. High resolution RGB image of the Gough Map. (a) is the whole map, where East is at the top of the page, north (Scotland) is to the left and England is to the right. Towns and distances are drawn in red; Ocean, coast and rivers are in green. Left 1/4 of the map is lamb skin and the rest is sheepskin. Note the damaged area at the right edge (south of Wales); (b) is a zoom window showing in red Hadrian's Wall, town signs, texts and green rivers; (c) shows the six overlapping chips of the data collection.

3.2. Results of Each Step

Details of each step will be introduced in the following subsections.

3.2.1. Extract water pixels

After cutting each HSI into sub-chips, we use the Mahalanobis distance classifier in ENVI to classify each chip into three classes. Here, even though in the end we only

need the binary mask of “water (green) pixels” and “everything else”, to get most accurate mask, we classify all the pigments into as many classes as visually apparent. The other supervised classification methods in ENVI were tried, such as spectral angle mapper and maximum likelihood, however, we found the Mahalanobis distance classifier provides the most visually accurate mask.

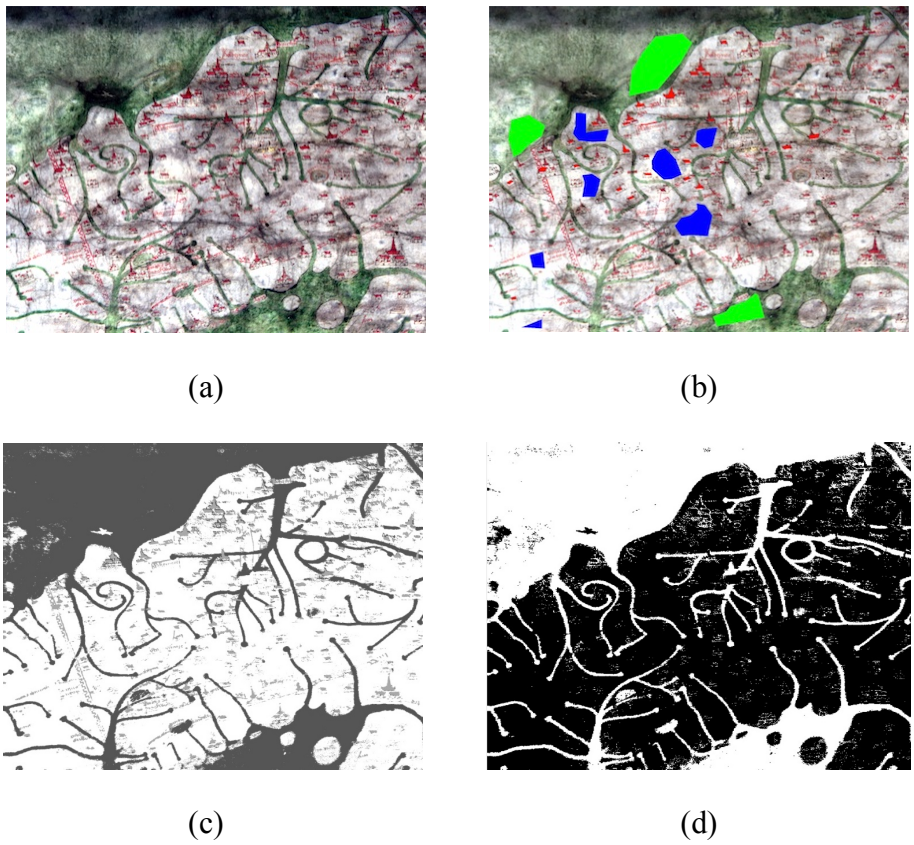

(a) (b)

(c) (d)

Figure 4. Process of extracting water pixels from one chip of the Gough Map. (a) Original RGB rendering of chip 2R (top); (b) Three regions of interest (ROI) specified in ENVI; (c) Three class classification result of the chip using Mahalanobis distance classifier; (d) Binary image with white pixels representing water pixels of the original image.

An example of the 2R(top) chip shown in Fig. 4(a), we first specify three regions of interest (ROI) as shown in Fig. 4(b), including red, green and blue (representing white). Then based on the three ROIs, we classify this chip into three classes shown in Fig. 4(c). We apply a threshold to convert (c) to a binary image shown in Fig. 4(d), so that

the white pixels in (d) represent all the water pixels in the original 2R(top) chip, automatically extracted. Finally, the data of water pixels are exported for endmember analysis and meanwhile, the coordinates of the water pixels are saved for future mapping.

3.2.2. Hyperspectral data pre-processing

The next step is data pre-processing, which includes sphering the data and spectrally binning the data. During the data collection, a white reference image for each HSI was also obtained. The white reference with essentially 100% reflectance is used to calibrate the instrument and to convert the image to estimated reflectance. The white reference material provides a Lambertian surface, which reflects light at all angles equally creating nearly perfect diffuse reflectance. By using the measured radiance of each pixel divided by the radiance of the white reference, we normalize out this white reference image to get the estimated reflectance of each pixel in the HSI. In this research, we focus on spectral differences between the water pigments instead of brightness differences. To ensure the same brightness levels for all of the chips, we sphere the data, i.e., normalize each pixel vector to a unit magnitude.

We also spectrally bin the data to increase the signal to noise ratio (SNR) and decrease the computation time. Previous research (Bai, Messinger, and Howell 2017b, a) showed that the pixels' spectral signatures are slowly varying in the spectral domain between 400nm and 1000nm. In order to boost the SNR, we spectrally bin each HSI chip by a factor of three, from 334 bands ($\Delta\lambda$ = 1.8 nm) to 111 bands (($\Delta\lambda$ = 5.4 nm).

3.2.3. Extract endmembers and estimate material diversity

After data pre-processing, we estimate the material diversity of the water pigments. We first use the MaxD to exact many endmembers and then use the Gram Matrix to decide

how many endmembers to keep. Fig. 5(a) depicts the estimated convex hull volume vs the number of endmembers of an example HSI chip (3L top) of the Gough Map and when the volume function approaches zero, the number of endmembers indicates the number of distinct materials in the HSI. The spectral reflectance of those six endmembers are plotted in Fig. 5(b). After applying the same method to the remaining image chips, we find that all of them have six distinct water pigments. The similarity in these results between different HSI chips is expected given the common materials and methods likely used across the entire map. However, the reflectance of the endmembers is not the same in different HSI chips indicating the need to compute global endmembers in the next section.

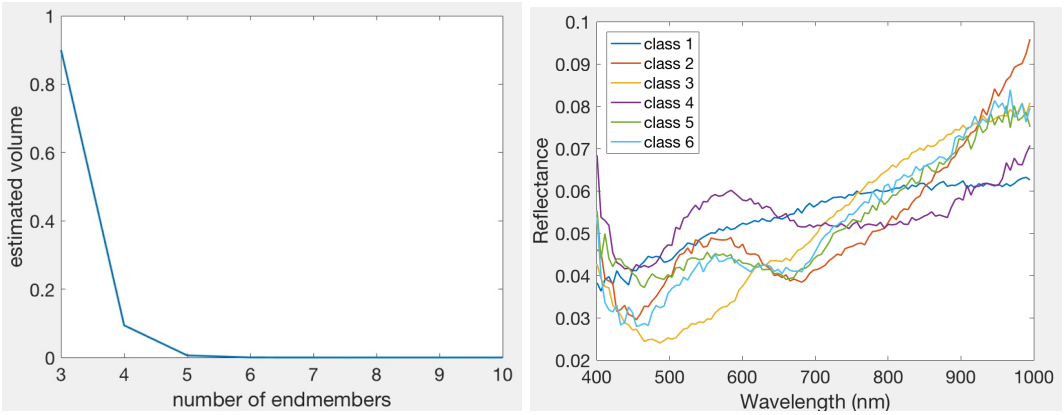

(a) (b)

Figure 5. Material diversity plot for chip 3L (top) of the Gough Map in (a), with x axis: number of endmembers and y axis: estimated convex hull volume. Reflectance of the endmembers for chip 3L (top) in (b), with x axis as wavelength in nm and y axis as reflectance.

3.2.4. Compute global endmembers

Given that each HSI chip has six endmembers, in total over the 12 chips we have 72 endmembers. In order to classify all the water pigments across the entire Gough Map, we need to compute global endmembers. Here, we use the Gram Matrix to estimate the

number of distinct water pigments based on the 72 primary endmembers. Similarly, the volume function depicts that there are six distinct water pigments over the entire Gough Map. Then, we use the K-means algorithm to classify the reflectance of those 72 endmembers into six clusters. Results are shown in Fig. 6 (a-f).

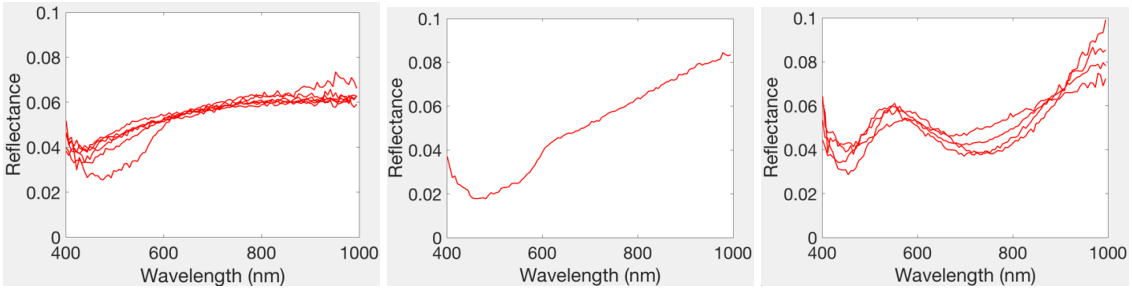

(a) (b) (c)

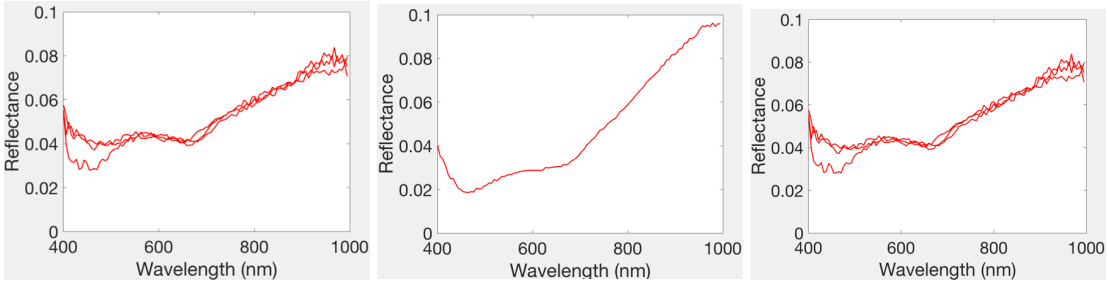

(d) (e) (f)

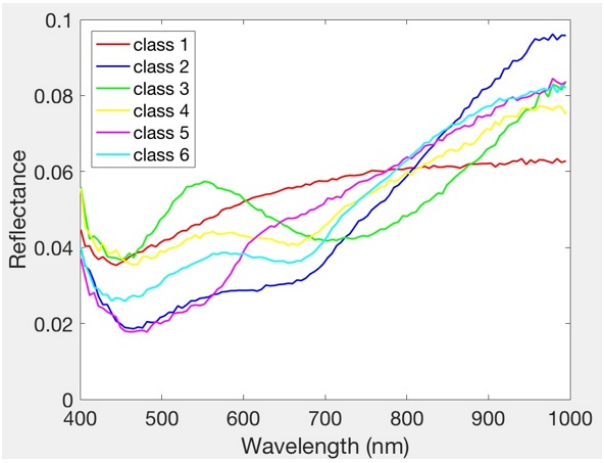

(g)

Figure 6. K-means classification results of 72 primary endmembers of the water pixels in (a-f) and averaged spectra of above six classes (g) representing six global endmembers in the Gough Map.

We compute the average spectrum within each cluster and the result is depicted in Fig. 6 (g). Notice that these six averaged spectra are distinct from each other and they represent six global distinct water (green) pigment endmembers across the entire Gough Map. Note that the endmembers are drawn from the data itself, and may not represent true green "pigments", but they do meet the mathematical description of endmembers as exemplar spectra in the high dimensional hyperspectral data space. However, the analysis only considered water pixels and so some resulting endmembers are not purely "green" but are included. The endmember in Fig. 6 (g) are different from the endmembers in Fig. 5 (b), which is because one single endmember from one chip is not a good representative of one distinct water pigment, indicating the need to compute an average reflectance after the clustering. Next, we apply an unmixing technique to separate the various contributions to each pixel. Note that in Fig. 6 (b) and (e), there is only one member of this class (taken from the original 72 endmembers). However, they are both spectrally unique and represented a distinct class.

3.2.5. Classify the water pixels per chip

Now we use NNLS to classify the water pixels based on the six global endmembers per chip. The output of NNLS is an abundance matrix, whose size is 6 (rows) x n (columns), where n is the number of pixels. Each column gives the proportion of the six endmembers in a single pixel. We also expand the abundance matrix into a new "abundances + differences" matrix, which includes the differences between each row of the abundance matrix. Then we use K-means to classify both the original abundance matrix and the "abundances + differences" matrix into six classes as described above. We assign the class label to each pixel according to the K-means results. After mapping the labels back to the image, we output the water pixel classification results in Fig. 7.

Due to the absence of the ground truth data, we will visually compare the classification results with the original RGB image. Comparing this result with Fig. 3(a) (the original RGB image of the Gough Map), we see that the water pigment in the ocean area is different from that in the coastal areas and waterways. The ocean area is likely painted with a mix of light and dark green ink and the coastal and waterways are drawn with a different kind of dark green ink and the faded area on the right looks even darker. The classification result visually matches the features of the original RGB image and it provides a spatial classification pattern of all the water pigments across the entire map. This will hopefully give historians more insight to its creation and revision.

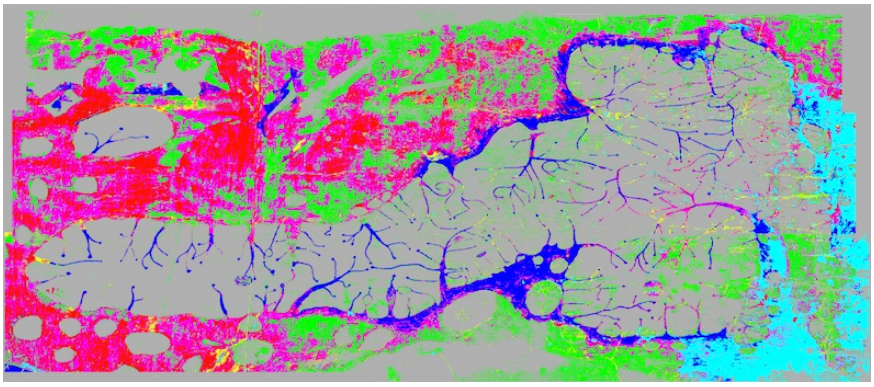

(a)

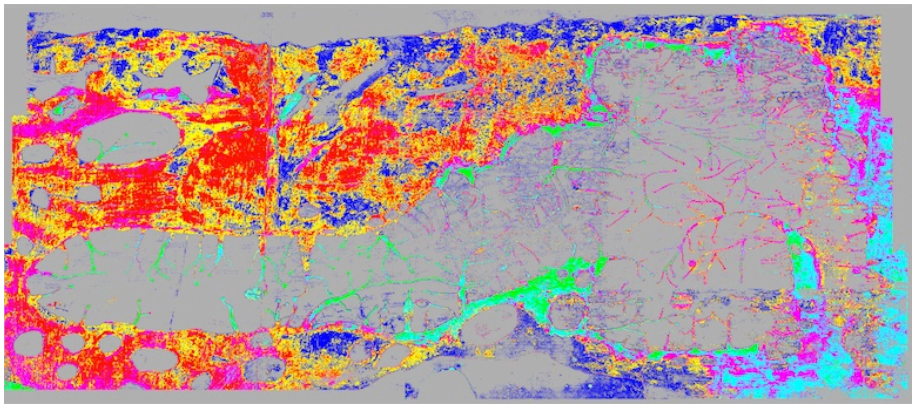

(b)

Figure 7. Classification results of HSI of the entire Gough Map (combination of 12 chips). (a) is the spectral unmixing result using NNLS + abundances. (b) is the spectral unmixing result using NNLS + abundances + differences.

3.2.6. Spectral angle spatial patterns

In this research, due to the absence of ground truth data, we use two different ways (NNLS + abundances and NNLS + abundances + differences) to classify the HSI of the Gough Map. The two methods convey similar classification results, but not exactly the same. It is desirable to validate the classification results as best as possible. Here, we use the spectral angle spatial pattern method to validate the results. This method intuitively shows the variability in each class and how similar the pixels in each class are to the class mean, a convenient measure of the quality of the class map in the absence of ground truth.

Figs. 8 and 9 depict the spatial patterns of the water pigments in six classes using two different methods: 1) NNLS + abundances, 2) NNLS + abundances + differences. The color bar shows the spectral angle ranging from 0 to 10 degrees. Discontinuities in the class map indicate individual pixels that may not be well represented by that specific class model, however, we are attempting to assess global patterns in the data as it is assumed the creators of the map applied the pigments in a relatively spatially contiguous manner.

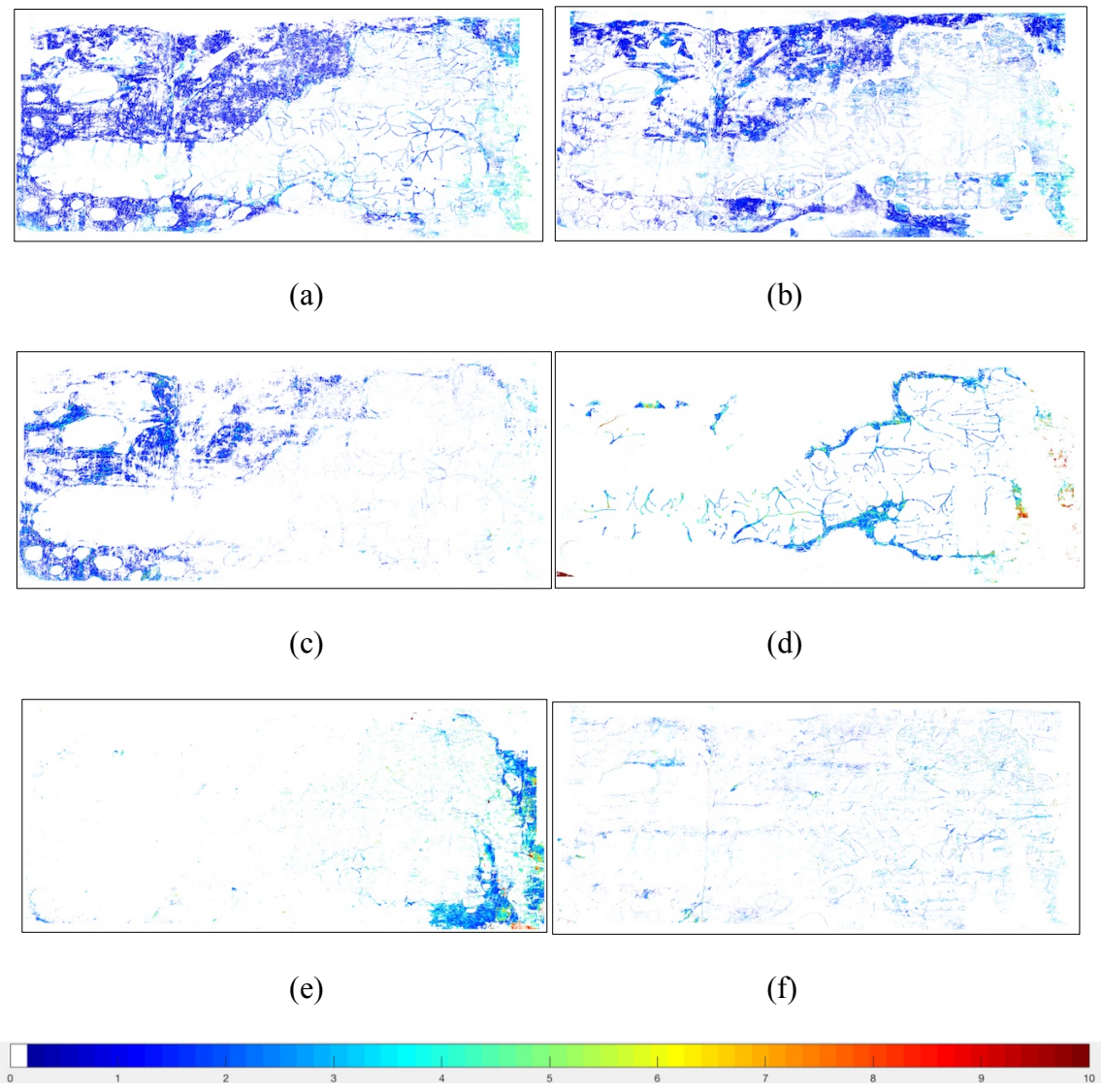

Figure 8. Spatial pattern of the spectral angles using NNLS + abundances within each class. (a) to (e) represent class 1 to 6 of the water pigment classification. (g) is the color bar ranging from 0 to 10.

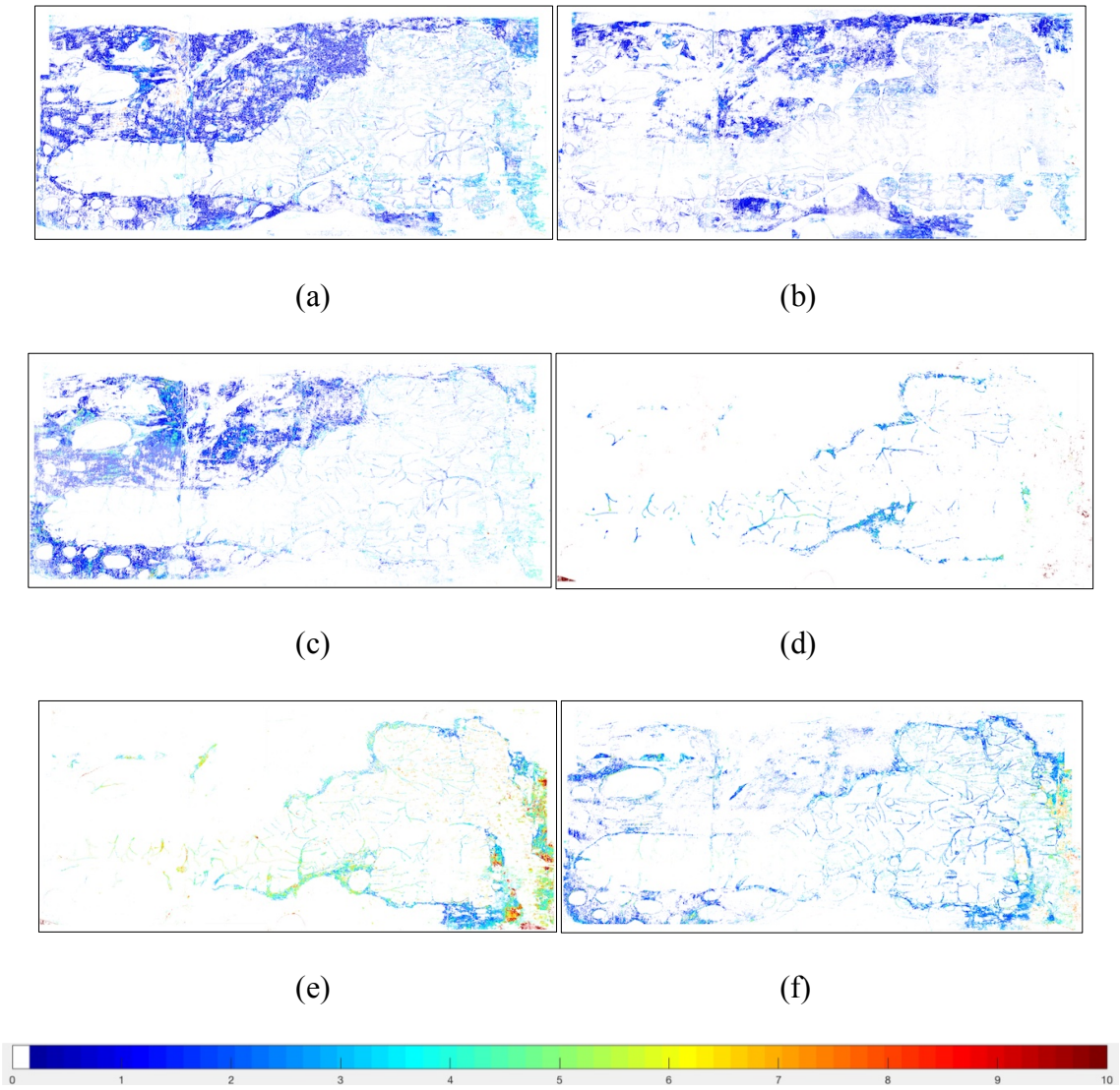

Figure 9. Spatial pattern of the spectral angles using NNLS + abundances + differences within each class. (a) to (e) represent class 1 to 6 of the water pigment classification. (g) is the color bar ranging from 0 to 10.

Notice that most of the patterns are only composed of blue and cyan indicating that the spectral angle is generally around 2-3 degrees. The right part of Fig. 9 (e) contains some large values indicating a poor match to the class average. The right part

of the original Gough Map was badly faded and changed. The water pigments there do not provide much useful information. In this case, we ignore those few red points with large spectral angle in the faded areas. Since the spatial patterns are generally good and there is not much variability in each class, we conclude that our classification results are acceptable.

4. Results for the Selden Map

This section introduces the application of the proposed method to classify the water pigments of the Selden Map.

4.1. Collection Parameters

The RGB image of the Selden Map is shown in Fig. 10 (a) and several zoom windows of the landmarks are shown in Fig. 10 (c). Notice the differences between the water pigments across the entire Selden Map. In 2015, this map was imaged using a hyperspectral system in 12 spatially overlapping HSI chips. We label them as chip 1 to 12 as shown in Fig. 10 (b). Note that chip 2 was lost during transmission. So that in the following figures, there will be a blank area in the map. All the calculations are based on remaining 11 chips. Similar to the HSIs of the Gough Map, the HSI chip of the Selden Map also has 334 spectral bands, ranging from 398.7 nm to 1000.3 nm ($\Delta\lambda$ = 1.8 nm). The spatial size of each chip varies from 1600 x 2300 (pixels) to 1600 x 3250 (pixels). Given the actual size of the map: 100cm x 160cm, its spatial resolution is about $\Delta x \approx \Delta y \approx 48$ pixels/cm (0.02 cm/pixel).

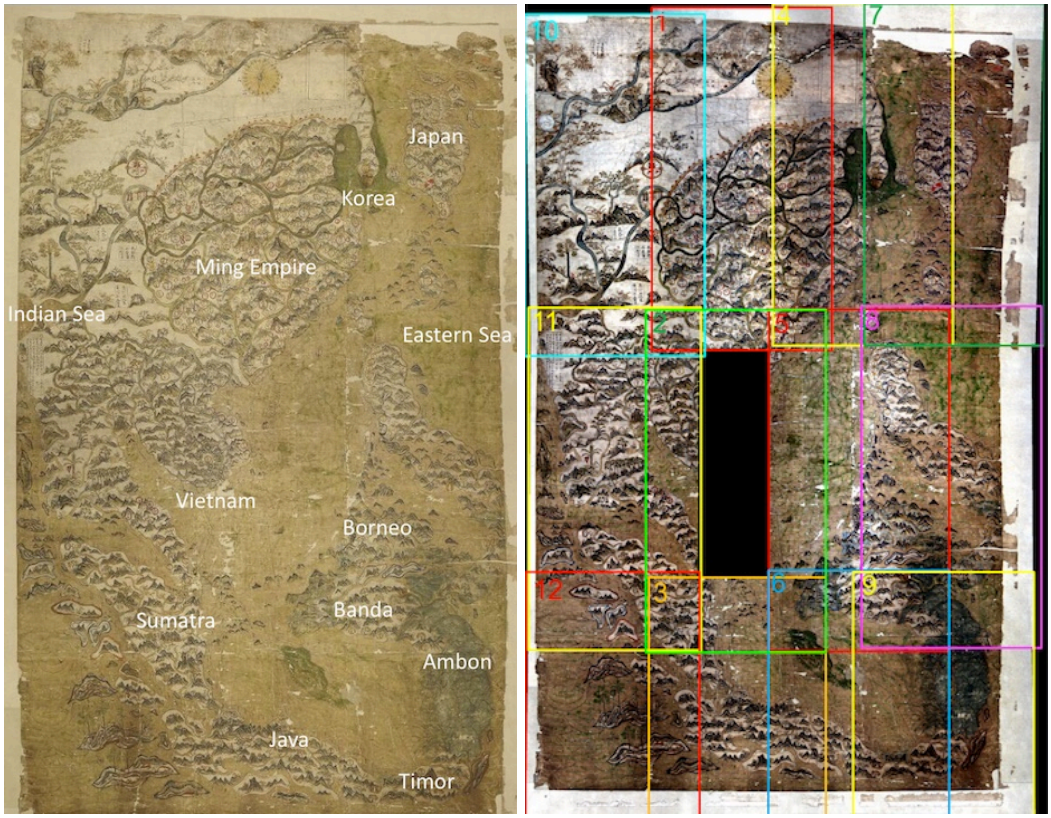

(a) (b)

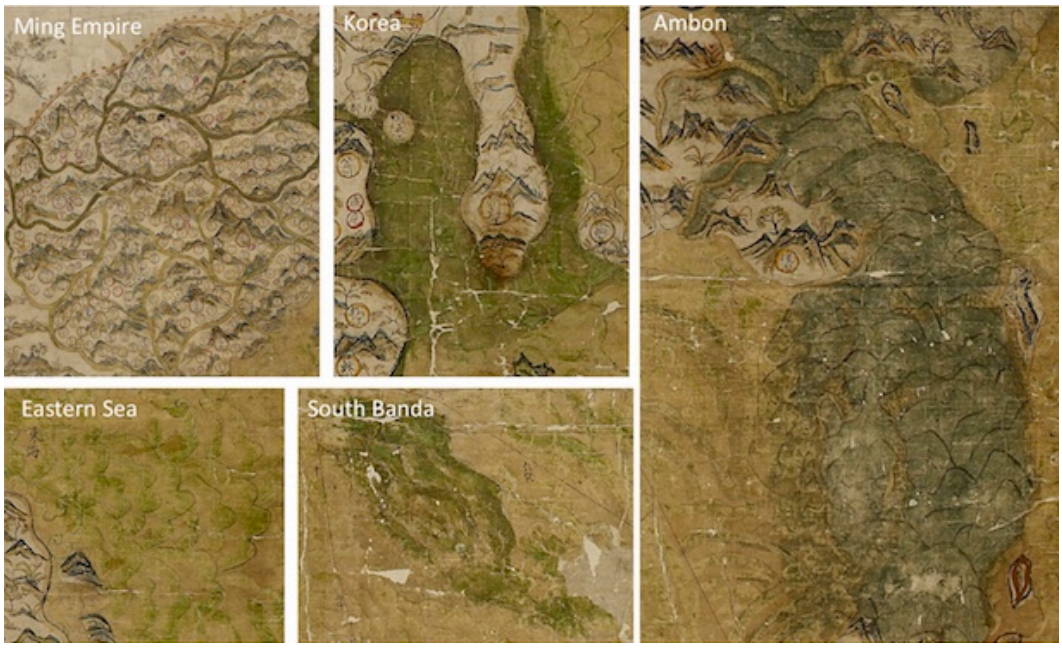

(c)

Figure 10. High resolution images of the Selden Map. (a) The RGB image of the entire map containing mountains, rivers, oceans, coastal routes, islands, cities and provincial

boundaries in different colors and patterns. The water (brownish green) pigment dominates this map; (b) RGB renderings of the HSIs representing the 12 overlapping chips of the Selden Map (chip 2 was lost); (c) Zoom windows of the landmarks with names labelled. Notice the differences between the water pigments.

4.2. Results of Each Step

We will follow the same procedure introduced in Section 2 to classify the Selden Map using the NNLS spectral unmixing method. However, due to the complexity of the pigments in the Selden Map, we extract the water pixels from the images by hand. The results of each step are provided in following subsections.

4.2.1. Extract water pixels

To accurately cover of all the water pixels, we use Photoshop to create a mask image. Fig. 11 shows an example process of extracting water pixels from chip 8 of the Selden Map. The original RGB rendering of the HSI chip is shown in Fig. 11 (a) and the water pixel mask is in Fig. 11 (b). The mask in Fig.11 (b) contains light green, dark green, brownish green and so on. Then we add a threshold to convert (b) to a binary image shown in Fig. 11 (c), so that the black pixels in (c) represent all the water pixels in the original chip, automatically extracted. The coordinates of those pixels are recorded for future mapping back into the image space.

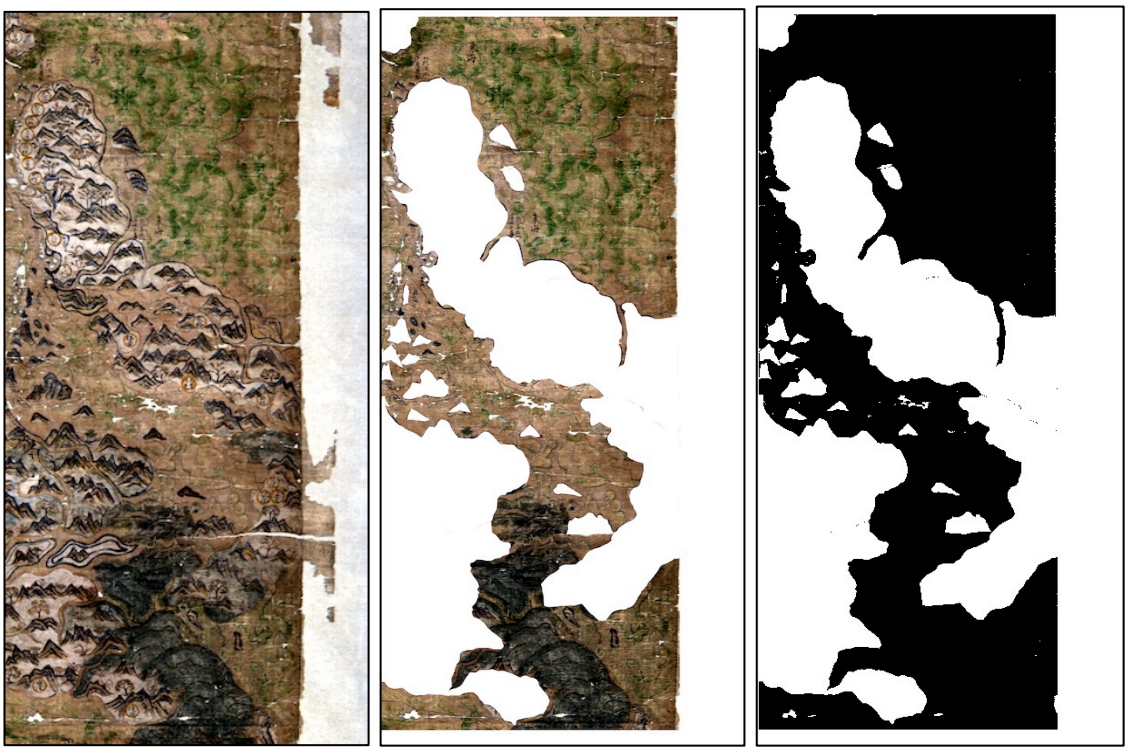

(a) (b) (c)

Figure 11. Process of extracting water pixels from one chip of the Selden Map. (a) Original chip 8 from the Selden Map; (b) Water pixels mask generated in Photoshop; (c) Binary image of (b) with black pixels representing water pixels in the original HSI.

4.2.2. Extract endmembers and estimate material diversity

After HSI pre-processing, including sphering the data and binning the data as before, we compute the MaxD to extract many endmembers and then use the Gram Matrix to decide how many endmembers to keep in each HSI chip. Note that we ignore chip 10 because there are very few water pixels in that chip. Here, we only analyze the remaining 10 HSI chips. The results indicate that there are six endmembers in each chip, so that in total we have 60 endmembers. An example results of chip 4 is shown in Fig. 12. Fig. 12 (a) indicates that there are six distinct water pixels in the HSI. The reflectance of those six endmembers are plotted in Fig. 12 (b).

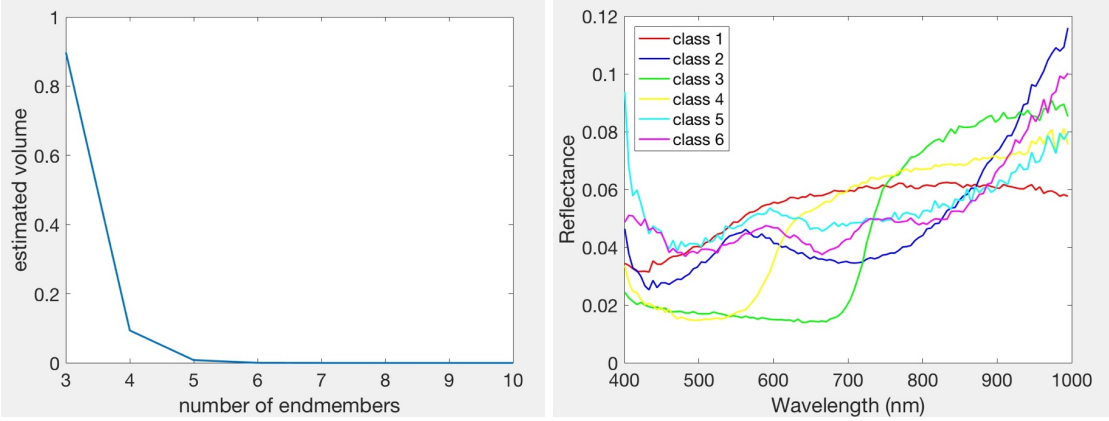

(a) (b)

Figure 12. Material diversity plot for chip 4 of the Selden Map in (a), with x axis: number of endmembers and y axis: estimated convex hull volume. Endmembers plot for chip 4 in (b), with x axis as wavelength in nm and y axis as reflectance.

4.2.3. Compute global endmembers

Now we use K-means to classify the 60 endmembers into six clusters. Results are shown in Fig. 13 (a-f). The averaged spectra of each cluster are shown in (g), which represent six global distinct water pigment endmembers in the Selden Map. The endmembers in Fig. 13 (g) are not necessarily the same as the endmembers in Fig. 12 (b). As discussed before, we need to compute an average spectrum within each class after K-means to provide the global distinct water pigment endmembers. Those global endmembers are used in the spectral unmixing to compute the abundances of those endmembers for all the pixels. As long as we have spectrally different global endmembers, the classes will be well separated, and class membership can be validated through analysis of the spatial pattern of the spectral angles between each pixel and its class mean. Note that some endmembers identified are not specifically "green" (i.e. Fig. 10d) but are still taken from water regions on the map.

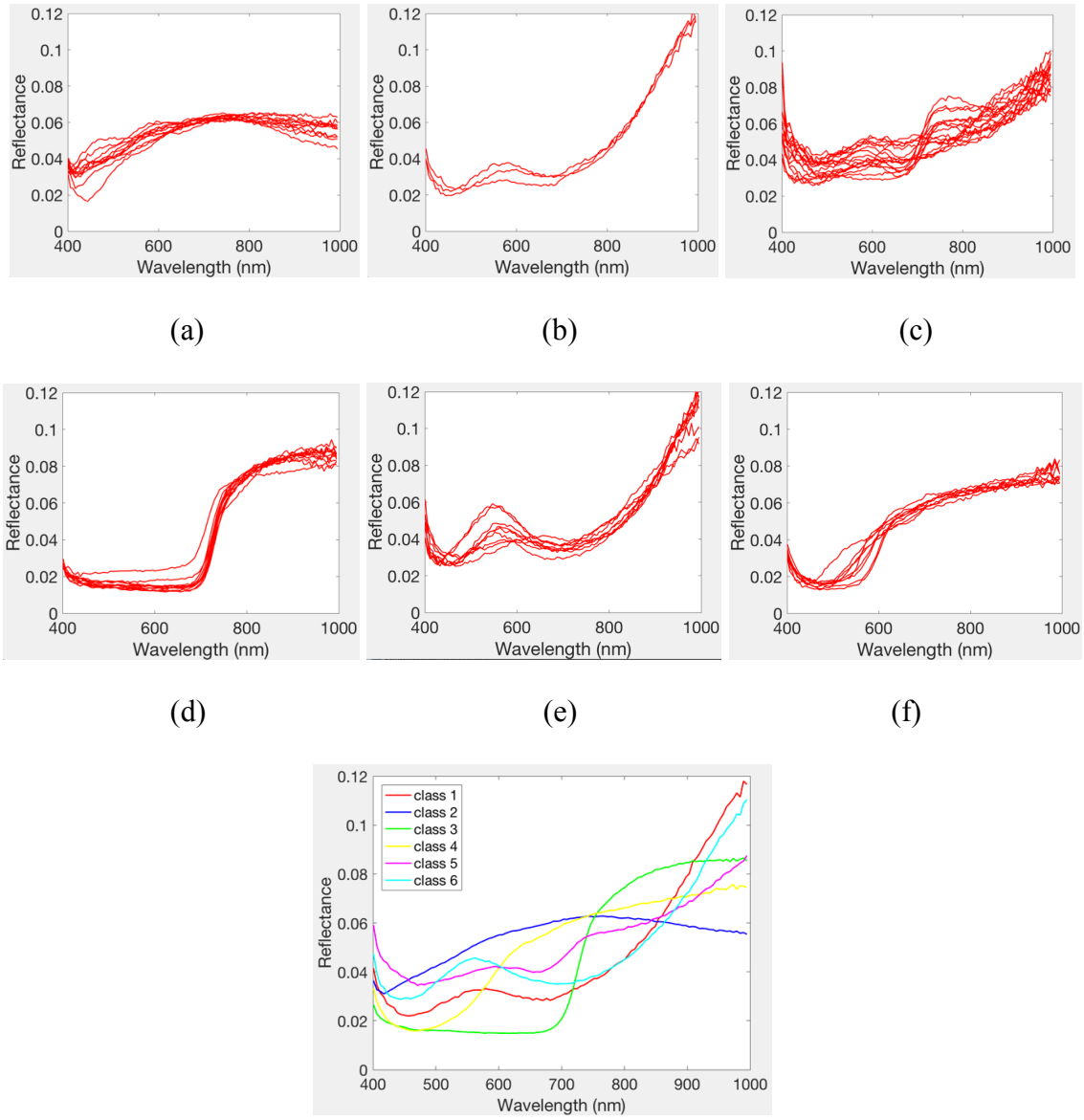

Figure 13. K-means classification results of 60 primary endmembers of the water pixels in (a-f) of the Selden Map and averaged spectra of above six classes (g) representing six global endmembers.

4.2.4. Classify the water pixels per chip

We use NNLS to classify the water pixels based on the six global endmembers per chip. After acquiring the abundance matrix and the "abundances + differences" matrix, we use K-means classification to label the pixels. The results are shown in Fig. 14. The

results of the two different methods may are similar but with a few differences. Since we do not have ground truth data for those maps, the similarity in the two results provides qualitative confidence in the resulting class maps.

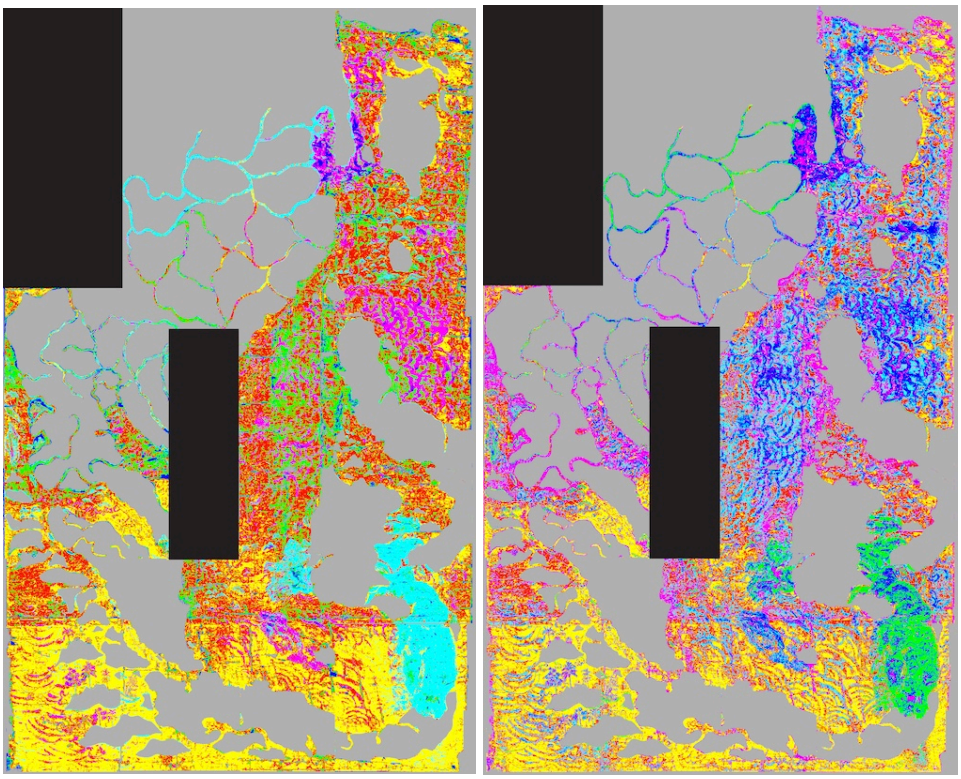

Figure 14. Classification results of the Selden Map (combination of 10 chips). (a) is the spectral unmixing result using NNLS + abundances; (b) is the result using NNLS + abundances + differences.

Notice that the green (water) pixels of the rivers are different in the south and north of the Ming Empire. Specifically, the green pixels in the north of Ming is the same as the green pixels in Ambon. The boundary of Korea is the same as the rivers of Ming, but different from those inside Korea. The green pixels inside Korea are similar to the land between Java and Banda. We can easily see the green waves in the Eastern Sea and find a folding line in the south of the Selden Map.

Previous study of the Selden Map revealed that the Selden Map was frequently displayed by the early 20th century (Minte et al. 2014) and by the 1970s, the map was

badly damaged according to the conservation records (Minte et al. 2014). After its rediscovery in 2008, Kogou et al (Kogou et al. 2016) found three different green pigments using an X - ray fluorescence (XRF) Spectrometer, including 1) indigo, 2) copper green (a basic copper chloride and possibly malachite) and 3) orpiment. Researchers argued that the oceans of the map were painted with an uneven brownish green (Kogou et al. 2016) and the wave patterns might have been blue before the copper pigment oxidised (Brook 2013). Batchelor found that there was a kind of darker green pigment used around Korea and the south and west of Borneo (Batchelor 2013). Specifically, in Borneo, the new sea color blotted out what was formerly a region of land (Batchelor 2013). The darker green in Ambon and Timor might be a correction that removed a former connection between them (Batchelor 2013).

Our classification result matches previous work and it significantly enriches the study of the Selden Map by providing a spatial classification pattern of all the water pigments as opposed to the point sampling of the XRF. These results give historians more insight on the map's creation, revision and even the transformation of the knowledge of the region.

4.2.5. Spectral angle spatial patterns

Figs. 15, 16 are the spectral angle spatial patterns of the map in six classes using two different methods: 1) NNLS + abundances, 2) NNLS + abundances + differences. Note that even though Fig. 15 (e) contains some points with large spectral angle, the class (e) does not provide much information about the water pigment diversity across the entire map, as most pixels in this class are in the boundaries of the oceans and mountains. This is due to the error when we create the water pigment mask. In this case, we ignore those few points. Since most of the spectral angles here are approximately 2-3 degrees, we

confidently conclude that our classification results are acceptable.

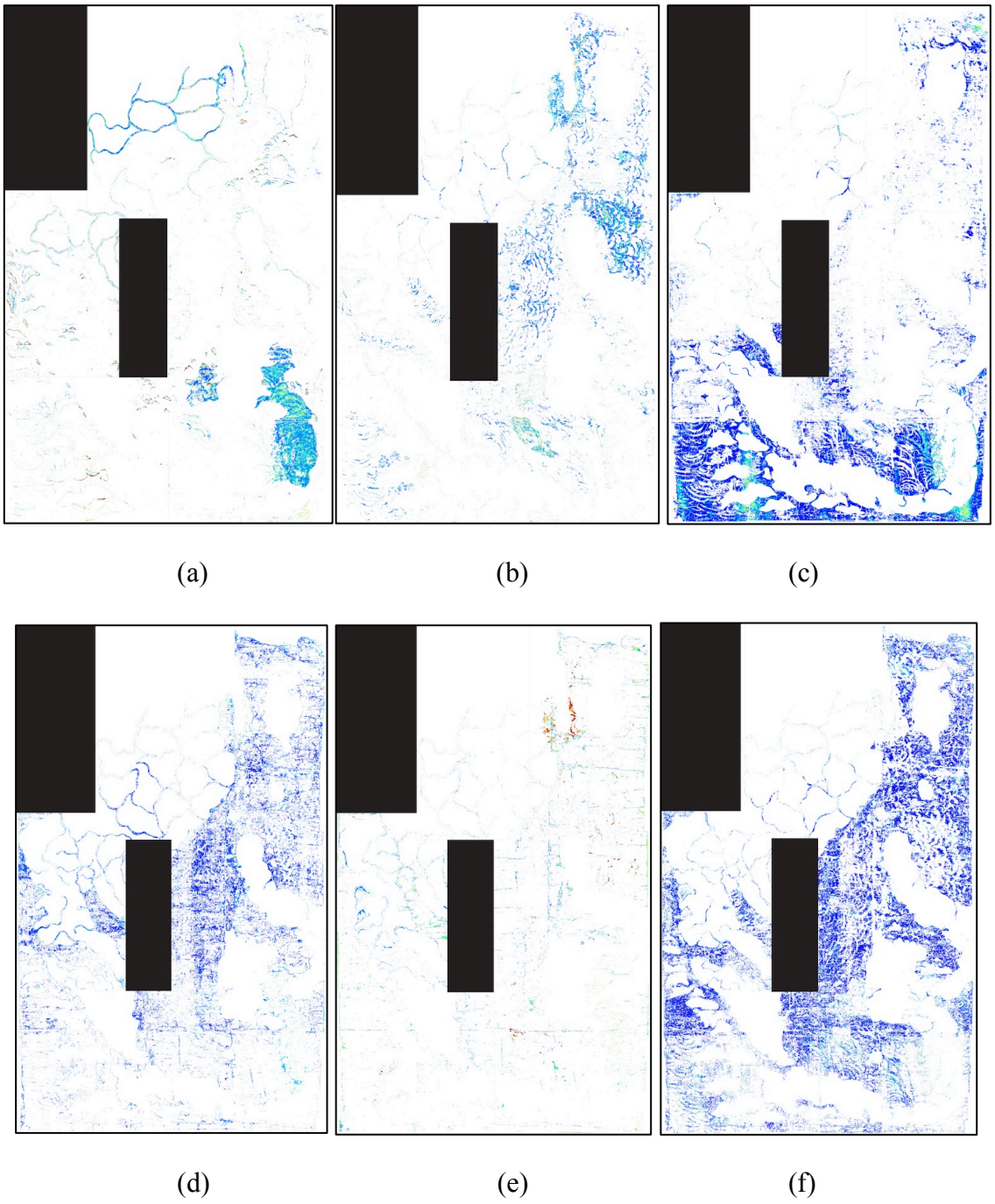

(a) (b) (c)

(d) (e) (f)

Figure 15. The Selden Map spatial pattern of the spectral angles using NNLS + abundances within each class. (a) to (e) represent class 1 to 6 of the water pixel classification. (g) is the color bar ranging from 0 to 10.

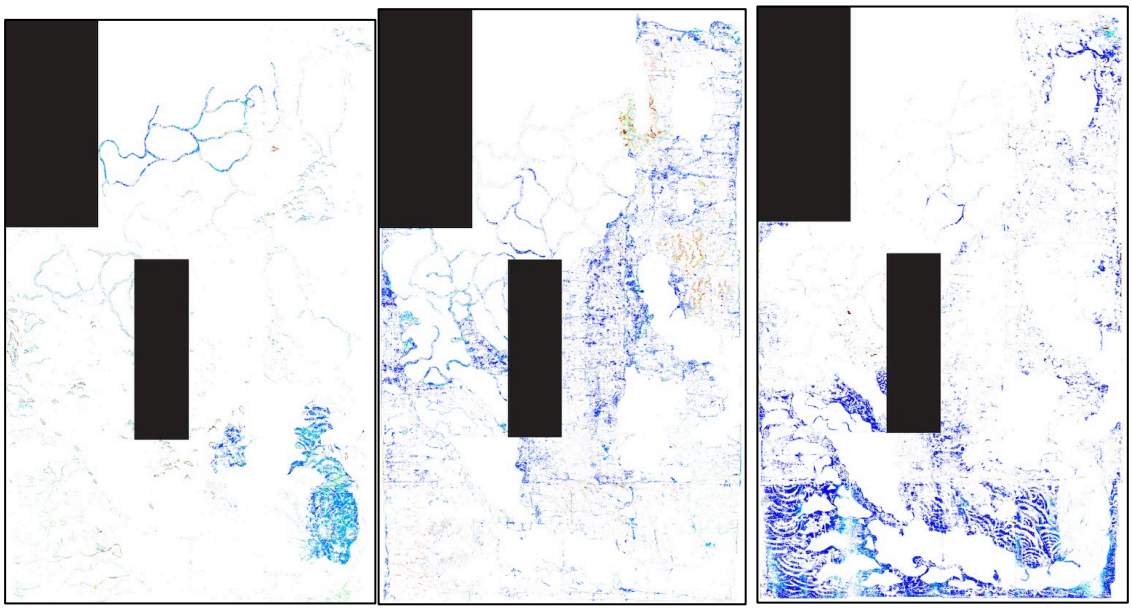

(a) (b) (c)

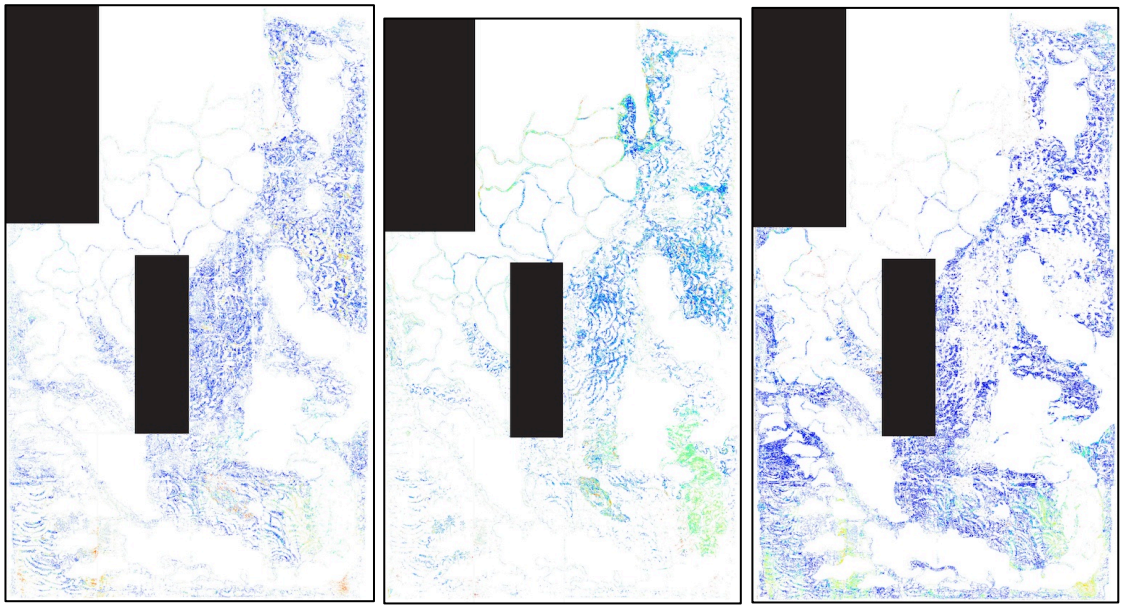

(d) (e) (f)

Figure 16. The Selden Map spatial pattern of the spectral angles using NNLS + abundances + differences within each class. (a) to (e) represent class 1 to 6 of the water pixel classification. (g) is the color bar ranging from 0 to 10.

5. Summary

This research provides a spectral unmixing based application for pigment analysis of medieval maps using hyperspectral imagery and provide insight into the spatial distribution of various pigments across these large artifacts. Two famous maps were imaged using a hyperspectral imaging system at the Bodleian Library, Oxford University in 2015. The Gough Map, dating from the 15th century, is one of the earliest surviving maps of Britain in geographically recognizable form. The Selden Map, dating from the 17th century, is one of the "Treasures of the Bodleian". Hyperspectral images provide both spatial and spectral information of these maps for the first time. In addition, the HSIs significantly enriched previous studies of medieval maps through global image analysis. The goal of this research is to estimate the green pigment diversity used to identify water in both maps and provide a global spatial pattern of the classification results. The Gram matrix and MaxD techniques are used to estimate the pigment diversity and extract the endmembers of each HSI chip. The NNLS spectral unmixing method is then used with K-means to classify all the water pigments into various classes. The endmembers are drawn from the data itself because mathematically, they are extrema points in the convex hull enclosing the data. They are not necessarily the "best" representation of a pure green pigment, but in the absence of ground truth, they do meet the mathematical description of endmembers as exemplar spectra in the high dimensional hyperspectral data space. Consequently, some extracted endmembers are expected to represent "pure" pigments, while others can be expected to represent mixtures that are unique in the high-dimensional data space. Especially, to validate the classification results, we compute the quality of the class assignment by calculation of the spectral angle between each pixel and its assigned class mean within each class. Given the dominant spectral angle is around 2-3 degrees, we are confident

that our classification results are acceptable.

The conclusion of this research contains two parts. For the Gough Map, we find six distinct water (green) pigments present in the map. There is a clear separation between the ocean area and the coast and waterways. For the Selden Map, there is a clear separation between north and south in the rivers of the Ming Empire. The green pigment of the rivers in the north is similar to that in Ambon and west of Banda. The pigment inside Korea is close to the land between Java and Banda. The green waves in the Eastern Sea and the folding line in the south of this map can be easily noticed. The classification results contribute to previous study by providing a spatial classification pattern of the water pigments across the maps. Apparently, the spatial distribution of the water pigments is related to the timeline of the construction and correction of the medieval maps. Historians will benefit from this research on the study of the maps' creation, revision and the transformation of the continent. In addition, the proposed class assigned validation method provides a good way to verify the classification results in circumstances, where ground truth is not available. This research can be generalized to a novel pigment mapping approach for historical geographers and cartographic historians to study the material diversity of historical artifacts by using hyperspectral imaging and consequently, contribute to the codicological study of cultural heritage artifacts.

Acknowledgements

The authors wish to acknowledge Dr. Robert Batchelor, Dr. Catherine Delano- Smith and Mr. Damien Bove for their insightful comments into the history, significance, and questions about the Selden map and the Gough Map. We also wish to acknowledge Mr. Nick Millea at the Bodleian Library, Oxford University for his assistance with this project.

Disclosure statement

No potential conflict of interest was reported by the authors.

Notes on contributors

Di Bai is a Ph.D. candidate at Chester F. Carlson Center for Imaging Science, Rochester Institute of Technology. He received his B.S. degree in graphic communication from Wuhan University in China and his MS degree in media sciences from Rochester Institute of Technology. His current research focuses on hyperspectral image analysis of cultural heritage artifacts and developing image processing tools for historical geographers and cartographic historians to analyze the timeline of creation of the artifacts. Address: Rochester Institute of Technology, Chester F. Carlson Center for Imaging Science, 54 Lomb Memorial Drive, Rochester, NY 14623, USA. Email: db3641@rit.edu

David W. Messinger received his bachelor's degree in physics from Clarkson University and his Ph.D. in physics from Rensselaer Polytechnic Institute. He is currently a professor, the Xerox Chair in Imaging Science, and director of Chester F. Carlson Center for Imaging Science, Rochester Institute of Technology. His personal

research focuses on projects related to spectral image analysis using physics-based approaches and advanced mathematical techniques. Address: Rochester Institute of Technology, Chester F. Carlson Center for Imaging Science, 54 Lomb Memorial Drive, Rochester, NY 14623, USA. Email: messinger@cis.rit.edu

David Howell received his B.Sc. in Chemistry from the University of East Anglia and his B.A. in English Mediaeval Studies from the University of Exeter. He is currently Head of Heritage Science at Bodleian Libraries, University of Oxford. His current research interests include the identification of materials in library collections using non-invasive analytical techniques and the revealing of hidden texts and obscured features in manuscripts. Address: University of Oxford, Bodleian Libraries, Broad St, Oxford OX1 3BG, UK. Email: david.howell@bodleian.ox.ac.uk

ORCID
Di Bai: http://orcid.org/0000-0002-5686-9843
David W. Messinger: http://orcid.org/0000-0002-2273-9194
David Howell: http://orcid.org/0000-0001-7257-1767

References

Attas, Michael, Edward Cloutis, Catherine Collins, Douglas Goltz, Claudine Majzels, James R Mans eld, and Henry H Mantsch. 2003. “Near-infrared spectroscopic imaging in art conservation: investigation of drawing constituents.” Journal of Cultural Heritage 4 (2): 127-136.

Bai, Di, David W Messinger, and David Howell. 2017a. “Hyperspectral analysis of cultural heritage artifacts: pigment material diversity in the Gough Map of Britain.” Optical Engineering 56 (8): 081805-081805.

Bai, Di, David W Messinger, and David Howell. 2017b. “A pigment analysis tool for hyperspectral images of cultural heritage artifacts.” In SPIE Defense+ Security, 101981A-101981A. International Society for Optics and Photonics.

Balas, Costas, Vassilis Papadakis, Nicolas Papadakis, Antonis Papadakis, Eleftheria Vaz-giouraki, and George Themelis. 2003. “A novel hyperspectral imaging apparatus for the non-destructive analysis of objects of artistic and historic value.” Journal of Cultural Heritage 4: 330-337.

Baronti, S, A Casini, F Lotti, and S Porcinai. 1998. “Multispectral imaging system for the mapping of pigments in works of art by use of principal component analysis.” Applied optics 37 (8): 1299-1309.

Barry, W. A. C., K. Boydston, and R. L. Easton. 2010. “Some Properties of Textual Heritage Materials of Importance in Spectral 27 Imaging Projects.” Vol. 1 of Proceedings of Eikonopoiia, Eikonopoiia, Digital Imaging of Ancient Textual Heritage: Technological Challenges and Solutions, Eikonopoiia, 27-38.

Barry, W. A. C., K. Boydston, and R. L. Easton. 2011. “Some Properties of Textual Heritage Materials of Importance in Spectral Imaging Projects.” Commentationes Humanarum Litterarum. 129: 35-50.

Batchelor, Robert. 2013. “The selden map rediscovered: a Chinese map of East Asian shipping routes, c. 1619.” Imago Mundi 65 (1): 37-63.

Batchelor, Robert K. 2014. London: The Selden Map and the Making of a Global City, 1549-1689. University of Chicago Press, Chicago, IL, USA.

Brook, Timothy. 2013. Mr. Selden's Map of China: Decoding the Secrets of a Vanished Cartographer. Bloomsbury Publishing, New York, USA.

Camastra, Francesco. 2003. “Data Dimensionality Estimation Methods: A Survey.” Pattern Recognition 36: 2945-2954.

Canham, K., A. Schlamm, A. Ziemann, B. Basener, and D. W. Messinger. 2011. “Spatially adaptive hyperspectral endmember selection and spectral unmixing.” IEE Trans. on Geo-science and Remote Sensing 49 (11).

Casini, Andrea, Franco Lotti, Marcello Picollo, Lorenzo Stefani, and Ezio Buzzegoli. 1999. “Image spectroscopy mapping technique for noninvasive analysis of paintings.” Studies in conservation 44 (1): 39-48.

Chen, Donghui, and Robert J Plemmons. 2010. “Nonnegativity constraints in numerical analysis.” In The birth of numerical analysis, 109-139. World Scientific, Hackensack, NJ, USA.

Cucci, Costanza, John K Delaney, and Marcello Picollo. 2016. “Reflectance hyperspectral imaging for investigation of works of art: old master paintings and illuminated manuscripts.” Accounts of chemical research 49 (10): 2070-2079.

Daniel, Floreal, Aurelie Mounier, Jose na Perez-Arantegui, C Pardos, N Prieto-Taboada, S Fdez-Ortiz de Vallejuelo, and K Castro. 2016. “Hyperspectral imaging applied to the analysis of Goya paintings in the Museum of Zaragoza (Spain).” Microchemical Journal 126: 113-120.

Delaney, John K, Mathieu Thoury, Jason G Zeibel, Paola Ricciardi, Kathryn M Morales, and Kathryn A Dooley. 2016. “Visible and infrared imaging spectroscopy of paintings and improved reflectography.” Heritage Science 4 (1): 6.

Delaney, John K, Jason G Zeibel, Mathieu Thoury, Roy Littleton, Michael Palmer, Kathryn M Morales, E Ren de la Rie, and Ann Hoenigswald. 2010. “Visible and

infrared imaging spectroscopy of Picasso's Harlequin musician: mapping and identification of artist materials in situ." Applied spectroscopy 64 (6): 584-594.

Delano-Smith, C., P. Barber, D. Bove, C. Clarkson, P.D.A. Harvey, N. Millea, N. Saul an W. Shannon, C. Whittick, and J. Willoughby. 2016. "New Light on the Medieval Gough Map of Britain." Imago Mundi 69:1: 1-36.

Dooley, Kathryn A, Suzanne Lomax, Jason G Zeibel, Costanza Miliani, Paola Ricciardi, Ann Hoenigswald, Murray Loew, and John K Delaney. 2013. "Mapping of egg yolk and animal skin glue paint binders in Early Renaissance paintings using near infrared reflectance imaging spectroscopy." Analyst 138 (17): 4838-4848.

Easton, R. L., W. A. C. Barry, and K. T. Knox. 2011. "Ten Years of Lessons from Imaging of the Archimedes Palimpsest." Commentationes Humanarum Litterarum. 129: 5-34.

Easton, R. L., and D. Kelbe. 2014. "Statistical Processing of Spectral Imagery to Recover Writings from Erased or Damaged Manuscripts." Manuscript Cultures. 7: 35-46.

Easton, R. L., K. T. Knox, and W. A. C. Barry. 2011. "Some Properties of Textual Heritage Materials of Importance in Spectral 27 Imaging Projects." Proceedings of the European Signal and Image Processing Conference, Eurasip, 1440-1444.

Easton, R. L., and W. Noel. 2004. "Multispectral Imaging of the Archimedes Palimpsest." Gazette du Livre Medieval. 45: 39-49.

Easton, R. L., and W. Noel. 2010. "Infinite Possibilities: Ten Years of Study of the Archimedes Palimpsest." Vol. 154 of Proceedings of the American Philosophical Society, 50-76.

Easton, R. L., K. Sacca, G. Heyworth, K. Boydston, C. V. Duzer, and M. Phelps. 2015. "Re-discovering text in the Yale Martellus Map, Spectral imaging and the new cartography." 7th IEEE International Workshop on Information Forensics and Security, 7th IEEE International Workshop on Information Forensics and Security.

Fischer, Christian, and Ioanna Kakoulli. 2006. “Multispectral and hyperspectral imaging technologies in conservation: current research and potential applications.” Studies in Conservation 51 (sup1): 3-16.

Goltz, Douglas, Michael Attas, Gregory Young, Edward Cloutis, and Maria Bedynski. 2010. “Assessing stains on historical documents using hyperspectral imaging.” Journal of cultural heritage 11 (1): 19-26.

Heylen, Rob, Mario Parente, and Paul Gader. 2014. “A review of nonlinear hyperspectral unmixing methods.” IEEE Journal of Selected Topics in Applied Earth Observations and Remote Sensing 7 (6): 1844-1868.

Jolli e, I.T. 2002. Principal Component Analysis. New York: Springer-Verlag New York.

Kirby, Michael. 2000. Geometric Data Analysis: An Empirical Approach to Dimensionality

Reduction and the Study of Patterns. New York, NY, USA: John Wiley & Sons, Inc.

Klein, Marvin E, Bernard J Aalderink, Roberto Padoan, Gerrit De Bruin, and Ted AG Steemers. 2008. “Quantitative hyperspectral reflectance imaging.” Sensors 8 (9): 5576-5618.

Knox, K. T., R. L. Easton, W. A. C. Barry, and K. Boydston. 2011. “Recovery of handwritten text from the diaries and papers of David Livingstone.” Vol. 7689 of Proceedings of the SPIE, Electronic Imaging.

Kogou, Sotiria, Sarah Neate, Clare Coveney, Amanda Miles, David Boocock, Lucia Burgio, Chi Shing Cheung, and Haida Liang. 2016. “The origins of the Selden map of China: scientific analysis of the painting materials and techniques using a holistic approach.” Heritage Science 4 (1): 28.

Kruse, F. A., A. B. Lefko , J. B. Boardman, K. B. Heidebrecht, A. T. Shapiro, P. J. Barloon, and A. F. H. Goetz. 1993. “The Spectral Image Processing System (SIPS) - Interactive Visualization and Analysis of Imaging Spectrometer Data.” Remote Sensing of Environment. 44: 145-163.

Lawson, Charles L, and Richard J Hanson. 1995. Solving least squares problems. Vol. 15. Siam, Philadelphia, PA, USA.

Legrand, Stijn, Frederik Vanmeert, Geert Van der Snickt, Matthias Alfeld, Wout De Nolf, Joris Dik, and Koen Janssens. 2014. “Examination of historical paintings by state-of-the-art hyperspectral imaging methods: from scanning infrared spectroscopy to computed X-ray laminography.” Heritage Science 2 (1): 13.

Liang, Haida. 2012. “Advances in multispectral and hyperspectral imaging for archaeology and art conservation.” Applied Physics A 106 (2): 309-323.

Lilley, K. D., C. D. Lloyd, and B. M. S. Campbell. 2009. “Mapping the Realm: A New Look at the Gough Map of Britain Cartographic Veracity in Medieval Mapping: Analyzing Geographical Variation in the Gough Map of Great Britain.” Imago Mundi 61:1: 1-28.

Melessanaki, K, V Papadakis, C Balas, and D Anglos. 2001. “Laser induced breakdown spectroscopy and hyperspectral imaging analysis of pigments on an illuminated manuscript.” Spectrochimica Acta Part B: Atomic Spectroscopy 56 (12): 2337-2346.

Messinger, D., A. Ziemann, A. Schlamm, and B. Basener. 2010. “Spectral image complexity estimated through local convex hull volume.” In 2010 2nd Workshop on Hyperspectral Image and Signal Processing: Evolution in Remote Sensing, June 1-4.

Messinger, David W., Amanda Ziemann, Bill Basener, and Ariel Schlamm. 2012. “Metrics of spectral image complexity with application to large area search.” Optical Engineering 51(3): 036201-1-036201-9. http://dx.doi.org/10.1117/1.OE.51.3.036201.

MILLEA, NICK. 2007. The Gough map: the earliest road map of Great Britain. Oxford: The Bodleian Library.

Minte, Robert, Marinita Stiglitz, Keisuke Sugiyama, and Mark Barnard. 2014. “From Quanzhou, China to Oxford, UK: an account of the Selden map of China and its conservation.” Studies in Conservation 59 (sup1): S115-S118.

Nie, H. 2014. “The Selden map of china: a new understanding of the Ming dynasty.”.
Pettis, K. W., T. A. Bailey, A. K. Jain, and R. C. Dubes. 1979. “An Intrinsic Dimensionality

Estimator from Near Neighbor Information.” IEEE Transactions on Pattern Analysis and Machine Intelligence PAMI-1 (1): 25-37.

Polak, Adam, Timothy Kelman, Paul Murray, Stephen Marshall, David JM Stothard, Nicholas Eastaugh, and Francis Eastaugh. 2017. “Hyperspectral imaging combined with data classification techniques as an aid for artwork authentication.” Journal of Cultural Heritage 26: 1–11.

Rosi, Francesca, Costanza Miliani, Ren Braun, Roland Harig, Diego Sali, Brunetto G Brunetti, and Antonio Sgamellotti. 2013. “Noninvasive analysis of paintings by mid-infrared hyperspectral imaging.” Angewandte Chemie International Edition 52 (20): 5258-5261.

Solopova, E. 2012. “The Making and Re-making of the Gough Map of Britain: Manuscript Evidence and Historical Context.” Imago Mundi 64:2: 155-168.

Yao, Futian, and Yuntao Qian. 2009. “Band selection based Gaussian processes for hyperspectral remote sensing images classification.” 2009 16th IEEE International Conference on Image Processing (ICIP) 2845-2848.

Ziemann, Amanda K., David W. Messinger, and William F. Basener. 2010. “Iterative convex hull volume estimation in hyperspectral imagery for change detection.” Vol. 7695, 76951I -76951I -9. http://dx.doi.org/10.1117/12.850122.